DEVELOPING A SMALL-SIZE PROTOTYPE FOR SOLAR COOLING WITH ABSORPTION CHILLERS

Mahmoud; R. K.[1] and El Attar; M. Z. [2]

ABSTRACT

*A mixture of absorbent "water" and refrigerant "ammonia" fluids concentrated at 50% was used as a working fluid. The power source was a solar flat plate collector **FPC** with gross area of 1.90 m^2. The FPC accumulates the collected solar energy in the generator vessel by the ammonia-water mixture. Two coaxial steel cylinders worked as condenser and evaporator. The outer cylinder circulates water to cool the system condenser in the condensing process. In the evaporating process (chilling), the outer cylinder is kept empty of water and the condenser cylinder works as evaporator. Experimental testing of the solar is assisted chiller was carried out for the evaluation of the system components and the overall thermal performance. Experiments were conducted in the Agricultural Engineering Department, Faculty of Agriculture, Al-Azhar University, Assiut branch, Assiut governorates, Egypt. It was found that the maximum system **COP** was 0.12 (0.04 ton of refrigeration load). This system can be used to cool three kilograms of potatoes crop from 30 °C to 4 °C under the experiment conditions, and 18 kilograms of potatoes can be cooled to 20 °C under the same conditions. In the average performance, the generator FPC delivered a 14.3% of the total available solar energy in one day. Meanwhile, generator vessel delivers 98% of FPC thermal energy or 13% from the total, solar intensity to the condenser-evaporator set. Net energy of the system condenser reached 55% form the energy delivered form generator vessel, and equals to 4.43 % from the total solar intensity.*

Keywords: renewable energy, liquid flat plate collector, solar chilling.

[1] **Demonstrator, Ag. Eng. Dept., Col. Ag. Al-Azhar U., Assiut.**
[2] **Lecturer, Ag. Eng. Dept., Col. Ag. Ain-Shams U.**

INTRODUCTION

Post-harvest, physiological obstacles such as ethane production, respiration and microbial attack prohibits getting high quality horticultural products to market challenge. The quality and storage life of fruits and vegetables may be seriously compromised within a few hours of harvest. Bakker-Arkema et al. (1999) described the harvesting operation as a catastrophic event, removing the product from its source of food. They summarized ways to minimize product quality loss in maintaining slow growth, biological activity, and spread of microorganisms of product by lowest temperature that will not cause freezing or chilling injury. Lipinski et al. (2013) stated that removing field heat from agricultural products could double shelf life and reduce spoilage rates that often exceed 40% of horticultural crops and 20 to 30 % of grain and cereal crops in developing countries according to **FAO** statistics of year 2009 (fig. 1).

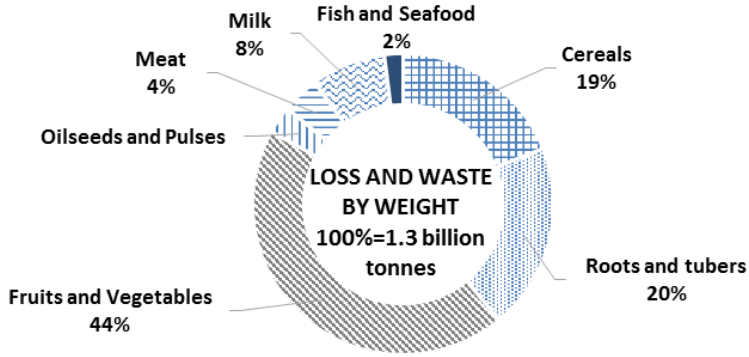

Figure 1: Losses Source: WRI analysis based on FAO. 2011. Global food losses and food waste-extent, causes and prevention. Rome: UN FAO (Cited form Lipinski, 2013).

To lower postharvest damage, the first aqueous-ammonia absorption refrigeration system was invented in Europe in 1815. Whitman et al. (2005) mentioned that the absorption water chillers use heat to drive the refrigeration cycle without having a mechanical compressor involved in the refrigeration cycle. Steam, hot water, or the burning of oil or natural gas are the most common energy sources for these types of chillers.

Wang (2000) remarked that vapor absorption cycle using water-ammonia systems was popular and widely used, but after the development of the vapor compression cycle it lost much of its

importance because of its low coefficient of performance (about one fifth of that of the vapor compression cycle).

Mittal et al. (2005) agreed that the air-conditioning system utilizing solar energy would generally be more efficient, cost wise, if it were used to provide both heating and cooling requirements. They noticed that various solar powered heating systems have been tested extensively, but solar powered air conditioning systems have received very little attention. The aim of this study is to investigate the potential and suitability of using solar energy as a source of power to drive a prototype of an agricultural vapor absorption chillier.

MATERIAL AND METHODS

The absorption cooling cycle (as shown in figure 2) performs in three phases: **1) Evaporation**, a liquid refrigerant evaporates in a low partial pressure environment, **2) Absorption**, the gaseous refrigerant is absorbed-dissolved into another liquid - reducing its partial pressure in the evaporator and allowing more liquid to evaporate. **3) Regeneration**, the refrigerant-laden liquid is heated, causing the refrigerant to evaporate out. It is then condensed through a heat exchanger to replenish the supply of liquid refrigerant in the evaporator.

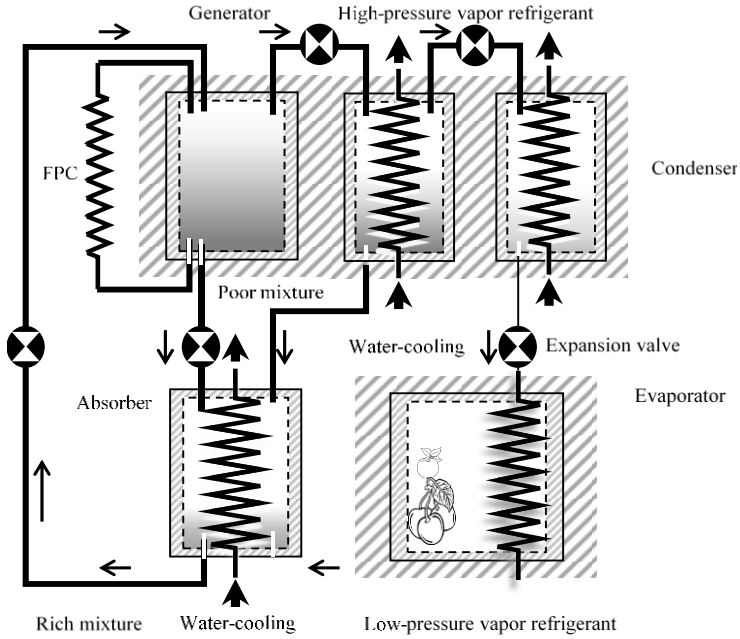

Figure 2: Principle and system description of the solar-operated chilling system.

Refrigeration cycle: vapor absorption refrigeration cycle -as shown in figure 3, consists in its basic configuration of a Solar Flat-Plate Collector (***FPC***) as thermal generator, condenser, evaporation, and absorber.

As mentioned by Kalogirou (2008), compared to an ordinary chilling cycle, the basic idea of an absorption system is to avoid compression work by using a suitable working pair. The working pair consists of a refrigerant, and a solution that can absorb the refrigerant.

A mixture of absorbent –water– and refrigerant-ammonia (R-717) ASHRAE 34 Class B2 - fluids concentrated at 50% was used as a working fluid (***WF***). Traditional criteria for selection of a refrigerant have involved a number of considerations, including efficiency, cost, operating pressures, toxicity, flammability, material compatibility and availability. In the generator, heat is supplied from the FPC to the fluids mixture in the generator vessel to drive off vapor refrigerant and, as a result, the remaining mixture becomes diluted, poor in refrigerant, and flows to the absorber. High-pressure vapor refrigerant flows to the condenser where it condenses to enter an expansion valve that reduces its pressure. The outlet of the expansion valve leads to the evaporator into which the liquid refrigerant flows and removes heat at low pressure turning into vapor again.

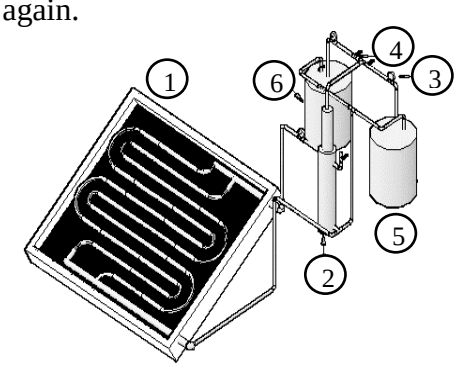

Figure 3: The solar refrigerator system: 1) flat plate solar collector, 2) generator vessel, 3) pressure gauges, 4) valve. 5) evaporator-condenser.

Generator: A solar flat-plate collector FPC was constructed and tested according to Abdel Mawla et al. (2012) in the Agricultural Engineering Department, Faculty of Agriculture, Al-Azhar University, Assiut branch, Assiut governorate, Egypt. Latitude 27.19 and longitude 31.18, with

14.08 hours day length and G_t = 8200 W.h/m^2 per day for solar declination angle of 23.41° (fig. 4).

Generator vessel was made of cylindrical steel pipe of 128 mm diameter, and 600 mm in height. The pipe was selected with 4 mm thickness to withstand high pressure resulting from vapor expansion. Generator vessel -as shown in figure 5 - leveled above the top of the FPC for circulating the fluids by gravitational force at desired flow rate.

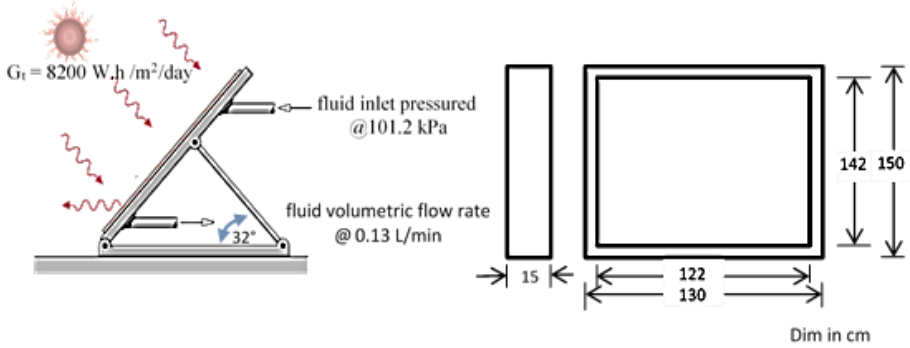

Figure 4: FPC overall dimensions constructed and tested at Assiut, Egypt.

Chiller condenser- evaporator consisted of two overlapping cylinders to represent the condenser and the evaporator vessels as shown in figure 6. Outer cylinder is 300 mm in diameter and 400 mm of length. The inner cylinder is 100 mm in diameter and cooled by running water in the outer cylinder space in the generation process. While in refrigeration process, the inner cylinder works as evaporator (without the cooling process and the outer cylinder is empty of water). The heat transfer coefficient was assumed independent of the fluid constant temperature.

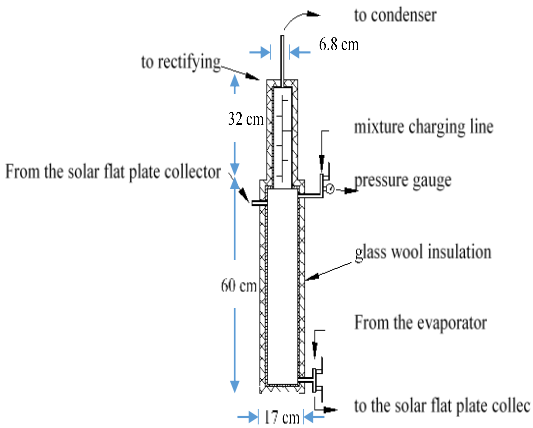

Figure 5: Generator storage vessel.

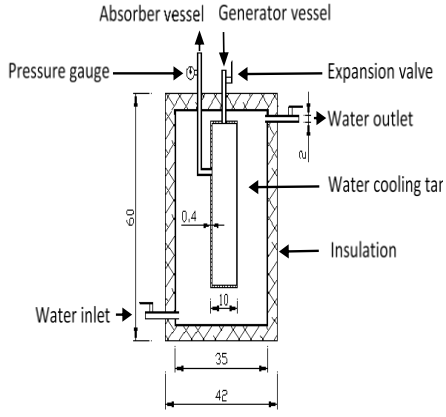

Figure 6: Condenser –evaporator.

System thermal analysis with composite systems, it is usual to work with an overall heat transfer coefficient **U**, which is defined by an expression analogous to Newton's law of cooling according to equation 1.

$$Q = U\ A\ \Delta T \qquad \textit{Equation 1}$$

The overall heat energy transfer coefficient ***U*** (showed in equation 2) is related to the total thermal resistance defining resistance ***R*** *"°K/W"* as the ratio of a driving potential to the corresponding transfer rate*;* equations 4, 13, and 14. A thermal resistance may also be associated with heat transfer by convection at a surface. From Newton's law of cooling as illustrated in equation 3.

$$U = \sum \frac{1}{AR} \qquad \textit{Equation 2}$$

$$Q = Ah(T_s - T_\infty) \qquad \textit{Equation 3}$$

$$R = \frac{L}{A\ k} \qquad \textit{Equation 4}$$

where **k** is the thermal conductivity "W/m °K", **h** is the heat transfer coefficients of surface"W/m^2 °K", **Ts** and $\mathbf{T}_\infty$ are the surface and ambient tempartures "°K", and **L** is the cross section of the tested material "m".

FPC generator thermal gain: FPC average temperature is difficult to measure through the different components and layers (fig. 7), which differs in its thermal properties, rather than evaluating the collector heat removal factor $\mathbf{F_R}$. Equation 7, describes $\mathbf{F_R}$ calculation. Reviewing equations 1 through 4, on the *FPC* can result in equations 5 through 8.

$$Q_u = Q_i - Q_o = G_t(\tau\alpha)A\text{-}U_{FPC}A_{FPC}(T_a - T_m) \qquad \textit{Equation 5}$$

$$Q_u = mC_p(T_{ho} - T_{ci}) \qquad \textit{Equation 6}$$

$$F_R = \frac{mC_p(T_{go} - T_{gi})}{A_{FPC}\left(G_t(\tau\alpha) - U_{FPC}(T_{gi} - T_m)\right)} \qquad \textit{Equation 7}$$

$$Q_u = F_R\ A_{FPC}\left(G_t(\tau\alpha) - U_{FPC}(T_{ci} - T_m)\right) \qquad \textit{Equation 8}$$

$$U_{FPC} = \sum \frac{1}{A_{FPC}\ R_{FPC}} \qquad \textit{Equation 9}$$

where $\mathbf{Q_u}$ is the FPC useful energy gain "W/m^2",$\mathbf{Q_i}$ is the FPC energy gain "W/m^2", $\mathbf{Q_o}$ is the FPC overall energy losses "W/m^2"**, m** is the WF mass flow rate "liters/s",**m** is the mass of WF in the storage tank "kg', $\mathbf{C_p}$

is the WF heat capacity "kJ/kg °K", $\mathbf{F_R}$ is the collector heat removal factor, $\boldsymbol{\tau}$ is the transmittance of the FPC covers, $\boldsymbol{\alpha}$ is the absorptance of the FPC plate, $\mathbf{U}_{FPC}$ is the FPC overall heat transfer coefficient "J/m^2 s °C", $\mathbf{A_{FPC}}$ is the surface area of FPC "m^2",$\mathbf{T_{ci}}$, $\mathbf{T_{ho}}$ are the entrance and outgoing temperatures of the ***WF*** "°K", $\mathbf{T_a}$, $\mathbf{T_m}$ are the avrage temperatures of working fluid of the FPC and the ambient air temprature "°K", and $\mathbf{G_t}$ is the solar radiation flux "W/m^2 per day". *Generator vessel thermal gain* U_g is obtained from equation 12.

$$Q_{gv} = Q_U - Q_o \qquad \textit{Equation 10}$$

$$Q_{gv} = U_{gv}\, A_{gv}\, \Delta T \qquad \textit{Equation 11}$$

$$U_{gv} = \frac{1}{\frac{1}{h_1}+\frac{r_1 ln(r_2/r_3)}{k_{ins}}+\frac{r_1 ln(r_3/r_1)}{k_{gv}}+\frac{r_1}{r_2 h_2}+R_{overall}} \qquad \textit{Equation 12}$$

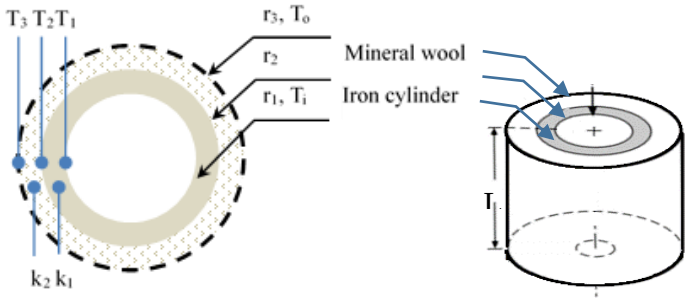

Figure 7: Heat transfer through layer of glass wool, and generator vessel surface.

where $\mathbf{Q_{gv}}$ is the WF absorbed energy in FPC during generation process, $\mathbf{U}_{gv}$ is the generator vessel overall heat transfer coefficient "J/m^2 s °C", $\mathbf{r_i}$ and $\mathbf{r_o}$ are the inner and the outer generator vessel radii "cm", $\mathbf{k_{ins}}$ is the thermal conductivity of insulation layer "W/m °K", $\mathbf{k_{ins}}$, $\mathbf{k_{gv}}$ are the thermal conductivities of insulation and the generator vessel "W/m °K", $\mathbf{h_1}$ and $\mathbf{h_2}$ are the heat transfer coefficients of the inner and outer generator vessel surfaces "W/m^2 °K", $\mathbf{A_{gv}}$ is the generator vessel exposed surface area "cm^2", $\mathbf{R_{overall}}$ is the overall thermal resistance "°K/W", and $\mathbf{r_1}$, $\mathbf{r_2}$, $\mathbf{r_3}$ are the inner and outer generator vessel, and insulation radii respectively "cm".

Condenser–Evaporator thermal gain: *Kassem et al.* (1993) described the energy of the evaporation according to the thermal load and desired cooling temprature (equations 13 and 14).

$$Q_e = W_P C_{PL}(T_{L\,max} - T_{L\,min}) \quad \textit{Equation 13}$$

$$Q_L = \frac{T_{ci} - T_{ho}}{\sum R_{overall}} \quad \textit{Equation 14}$$

where $\mathbf{Q_e}$ is the available chilling energy during refrigeration period - evaporator "kJ", $\mathbf{Q_L}$ is the magnitude of the heat removed from the refrigerated space at temperature $\mathbf{T_L}$, $\mathbf{R}_{\text{FPC overall}}$ is the overall thermal resistance "°K/W", $\mathbf{C_{pL}}$ is the specific heat of load material "k_j/kg", $\mathbf{W_p}$ cooled agricultural matieral mass "kg", $\mathbf{T_{Lmx}}$ is initial temperature of thermal load "°C", and $\mathbf{T_{Lmin}}$ is the minimum load temperature "°C",

Thermal analysis, system insulation and covers: Thermal insulations consist of low thermal conductivity materials combined to achieve an even lower system thermal conductivity. Wood and glass wool were used as thermal insulation of the system and the total resistance was calculated according to the following equations:

$$R_{FPC} = R_{covers} + R_{glass\,wool} + R_{wood} + R_{comb} \quad \textit{Equation 15}$$

$$R_{FPC} = \sum \frac{1}{A_{FPC}\ U_{FPC}} = \frac{X_{wool}}{A_{FPC}\,K_{wool}} + \frac{X_{wood}}{A_{FPC}\,K_{wood}} + \frac{1}{h_{comb}\,A_{FPC}} \quad \textit{Equation 16}$$

where $\mathbf{K_{wood}}$ the thermal conductivity of the wooden frame material "W/m °K", and $\mathbf{x}_{\text{wood}}$, $\mathbf{x}_{\text{wool}}$ are the thicknesses of wood and glass wool "cm".

Generator FPC thermal losses: Heat transfer through construction and insulation materials may include several modes: conduction through the solid materials; or convection through the air in the void spaces; and radiation exchange between the surfaces of the solid matrix

$$h_{rad} = \frac{\dot{Q}_{rad}}{A(T_s - T_a)} = \varepsilon\sigma(T_{\infty 2}^2 + T_2^2)(T_2 + T_{\infty 2}) \quad \textit{Equation 17}$$

$$h_{conv} = \frac{1}{RA} \quad \textit{Equation 18}$$

$$h_{comb} = h_{conv} + h_{rad} \quad \textit{Equation 19}$$

where $\mathbf{h}_{\text{conv}}$ is the convection heat transfer coefficient "W/m^2 °K", $\mathbf{h}_{\text{rad}}$ radiation heat transfer coefficient "W/m^2" , $\mathbf{h}_{\text{comb}}$ combined convection and radiation heat transfer coefficient "W/m^2 °K", $\boldsymbol{\varepsilon}$ is the emissivity, $\mathbf{Q_{rad}}$ is the radiation energy, $\boldsymbol{\sigma}$ is the Stefan-Boltzmann constant (5.67×10^8 W/m^2 K^4), $\boldsymbol{\varepsilon}$ is a radiative property of the surface termed the

emissivity, $\mathbf{T_s}$ is the material surface temperature, $\mathbf{T_a}$ is the ambient air temperature, and $\mathbf{T}_\infty$ fluid temperatures.

Generator and condenser–evaporator vessels thermal losses: Thermal losses can be estimated with equations 20 through 22,

$$R = R_{conv} + R_{cyl} + R_{ins} + R_{conv} + R_{rad} \quad \textit{Equation 20}$$

$$R = R_{conv} + R_{cyl} + R_{ins} + R_{comb} \quad \textit{Equation 21}$$

$$R = \frac{1}{2\pi r_i L h_i} + \frac{Ln\frac{r_2}{r_1}}{2\pi K_1 L} + \frac{Ln\frac{r_3}{r_2}}{2\pi K_2 L} + \frac{1}{2\pi r_o L h_0} + \frac{1}{\pi D^2 h_{rad}} \quad \textit{Equation 22}$$

where $\mathbf{R_{conv}}$ is the thermal resistance by convection "°K/W", $\mathbf{R_{cyl}}$ is the thermal resistance of the vessel "°K/W", $\mathbf{R_{ins}}$ is the thermal resistance of the insulation layer "°K/W", $\mathbf{R_{rad}}$ are the thermal resistance equivlent radiation "°K/W", $\mathbf{R_{comb}}$ is the combined thermal resistance "°K/W", $\mathbf{r_i}$, $\mathbf{r_o}$ is the outer and inner layers of insulation "°K/W", $\mathbf{r_o}$, $\mathbf{r_i}$ are the cylinder inner and outer radii "cm", **L** is the length of the clendrical generator vessel "cm", and $\mathbf{k_n}$ is the thermal conductivity of nth layer of insulation "W/m.°K".

FPC generator efficiency ($\boldsymbol{\eta_{FPC}}$) is a ratio of gained energy by the vessel heat exchanger $\mathbf{Q_{gv}}$ to the input thermal energy $\mathbf{Q_u}$ (stated in equation 8) gained from the FPC. The generator vessel efficiency $\boldsymbol{\eta_{gv}}$, was calculated Duffie and Beckman (2013) and Kalogirou (2004) as cited in equations 23 and 24.

$$\eta_{FPC} = \frac{\int Q_U dt}{A_{FPC} \int G_t dt} \quad \textit{Equation 23}$$

$$\eta_{FPC} = F_R(\tau\alpha) - F_R U_{FPC} \left(\frac{T_{gi} - T_m}{G_t}\right) \quad \textit{Equation 24}$$

Generator vessel efficiency ($\boldsymbol{\eta_g}$) is a ratio of gained energy by the vessel heat exchanger $\mathbf{Q_{gv}}$ to the input thermal energy $\mathbf{Q_u}$ (equation 8) gained from the FPC, $\mathbf{T_c}$ *is the temperature of the WF "°K",* $\mathbf{T_m}$ *is the temperature of the ambient still air "°K".* The generator vessel efficiency $\boldsymbol{\eta_g}$, was calculated according to equation $\mathbf{T_{go}}$ *is the WF temperatures in the generator at the end of each cycle "°K", and* $\mathbf{T_{gi}}$ *is the WF temperatures in the generator at the beginning of each cycle "°K"*

$$\eta_g = \frac{Q_{gv}}{Q_u} \quad \textit{Equation 25}$$

Condenser –Evaporator efficiency (η_{ce}): In each performed experiment, the temperature of the cold fluid (water) and the hot vapor of ammonia was recorded and the efficiency of the condenser was estimated by Helmut Wolf (1983) equation for heat transfer (equation 26).

$$\eta_{ce} = (\frac{T_{co}-T_{ci}}{T_{hi}-T_{ci}})100 \qquad \textit{Equation 26}$$

*where T_{co} is the condenser WF outlet temperature "°K", T_{ci} is the condenser **WF** inlet temperature "°K", and T_h is the temperature of hot **WF** "°k".*

System overall efficiency, Cengel (2007) defined the coefficient of performance *COP* as the heat load in the evaporator per unit of heat load in the generator (equation 27). The analysis was submitted according to El Masry (2002) and Eicker (2006) as shown in equations 28 and 29.

$$Coefficient\ of\ Performance\ (COP) = \frac{desired\ output}{required\ input} \qquad \textit{Equation 27}$$

$$COP_{cooling} = \frac{refrigration\ rate\ (Q_e)}{rate\ of\ heat\ addition\ to\ generator\ (Q_g)} \qquad \textit{Equation 28}$$

$$Q_{cold} = \eta_{FPC} . (COP)_{cycle} \qquad \textit{Equation 29}$$

Figure 8 describes the chilling process. **Generation** phase as illustrated in figure 8a starts by closing valves **I**, **III** and **V**, while valve **I** is opened. The FPC thermal gain causes the ammonia-water mixture to heat up. Circulating the mixture up the pipes to the generator storage vessel. Ammonia vapor rises out of solution through the rectifying column and into condenser where ammonia vapor condenses. At the end of the generation phase, the condenser is isolated from the generator by closing valve **I** and the temperature of the system allows cooling to ambient conditions.

The **refrigeration** phase – figure 8b– started by opening valve **III** so liquefied ammonia in the evaporator vaporizes back to the absorber and extracting heat form the evaporator space. Resulted ammonia vapor redirected to be absorbed in the weak solution stored in the generator vessel.

Solar radiation intensity was measured in all experiments by a Pyranometer model PSP with sensitivity of 9 µV per W/m^2, and ±0.5% linearity. Measurements ranged from 0 to 2800 W/m^2. A digital

thermocouple type K with measurement range varied from 200 to 1250 °C. Recorded system temperatures. System fluids and their mixture flow rate was measured by the volume-time method. Fluid volumes were measured with 500 ml glass cup with ±4 accuracy at 20 °C, and time was recorded by a digital stop-watch accurate to 1/60 s. System pressure was measured by three stainless steel 25 bar pressure gauges. The system ambient air speed was measured by a cup-counter type anemometer with accuracy of 1 m/s (±5%) in the measuring range 1- 67 m/s.

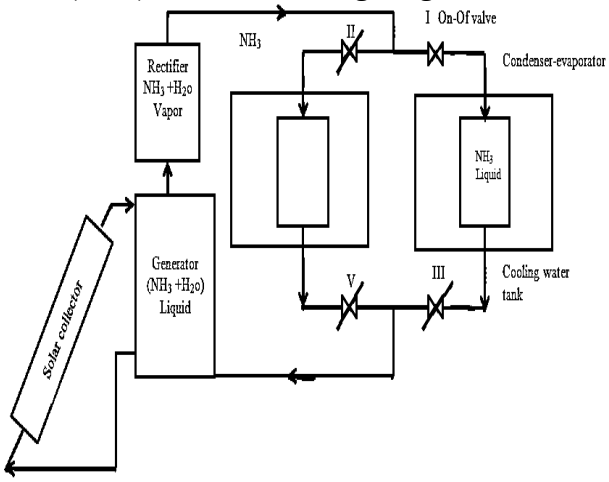

a-Generation

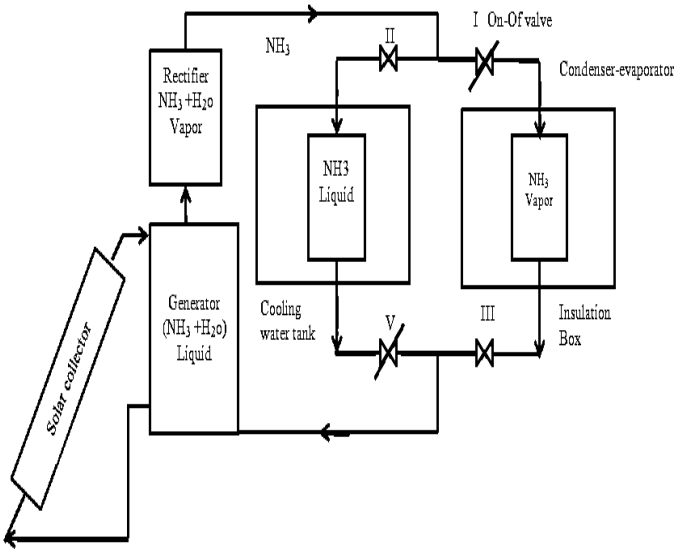

b- Refrigeration

Figure 8: Configuration of the experimental setup at a) generation and b) refrigeration process.

RESULTS AND DISCUSSION

Figure 9 illustrates the relationship of gained temperature of the working fluid measured at different times of the day. The relationship between the ***FPC*** and the absorber plate temperature T_P, and ammonia-water mixture temperature T_{aw} ***is shown in*** figure 10.

Generator: vessel thermal performance: To minimize thermal loss from generator vessel, a glass wool layer was used to cover the exposed surface of the generator vessel. Measurements were taken to calculate the amount of energy that passing through the generator. Figure 11, showed the energy delivered to the generator vessel from the generator FPC.

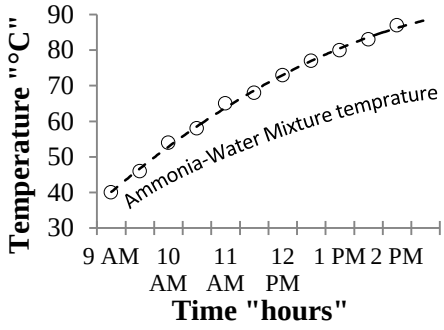

Figure 9: Daily temperature from the FPC to the working fluid in chilling system.

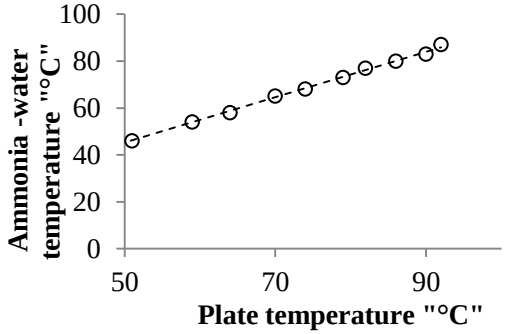

Figure 10: The relationship between the FPC absorber plate temperature and Ammonia-water temperature.

Increased temperature difference decreases the amount of useful energy passes through the generator vessel. The generator vessel heat transfer decreased from 98% to 22.8% with increased temperature difference from 9 to 44 °C.

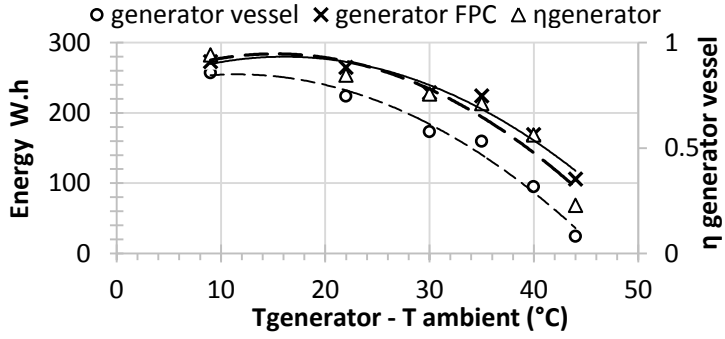

Figure 11: Heat transfer from the generator FPC to vessel in relation to temperature difference.

Condenser thermal performance: Results of this experiment indicated that the efficiency varied between 55 to 25% through the day. Figure 12 illustrates the energy gain from the generator vessel to the condenser as a function of the temperature difference of fluid.

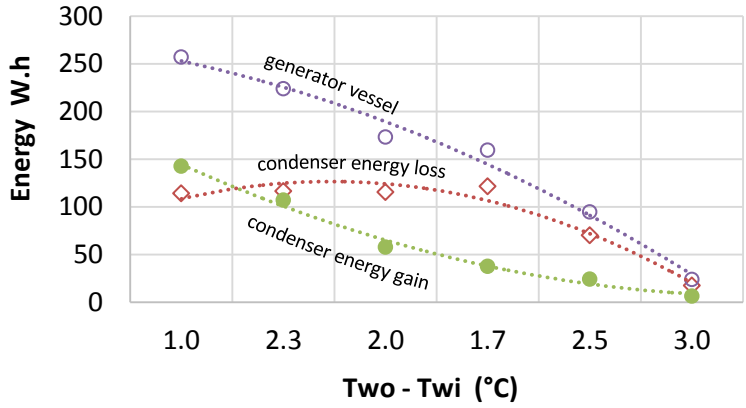

Figure 12: Heat transfer from generator vessel through condenser-evaporator.

Energy losses depend on the difference between inlet and outlet temperatures of the cold fluid and the difference between inlet temperature to each of cold and hot fluid during the process.Figure 13 shows that the system temperature changed according to solar intensity during one day of. The system pressure changed as a function of system energy (fig. 14).

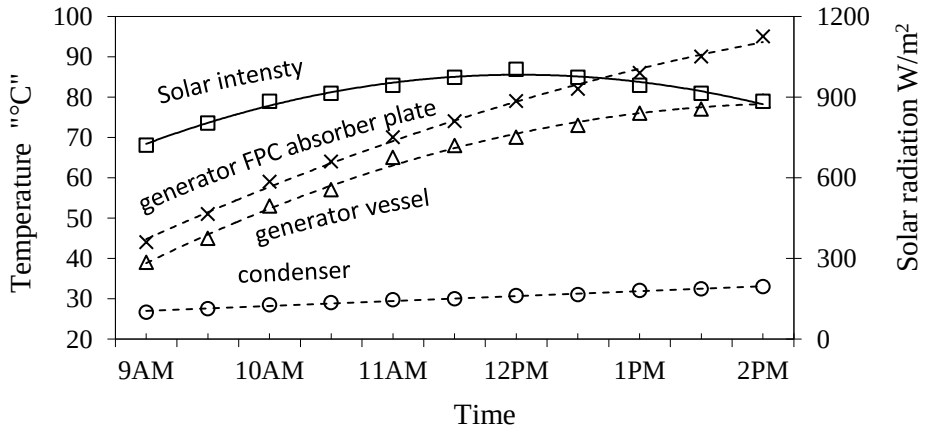

Figure 13: Heat transfer through chilling system at solar radiation intensities.

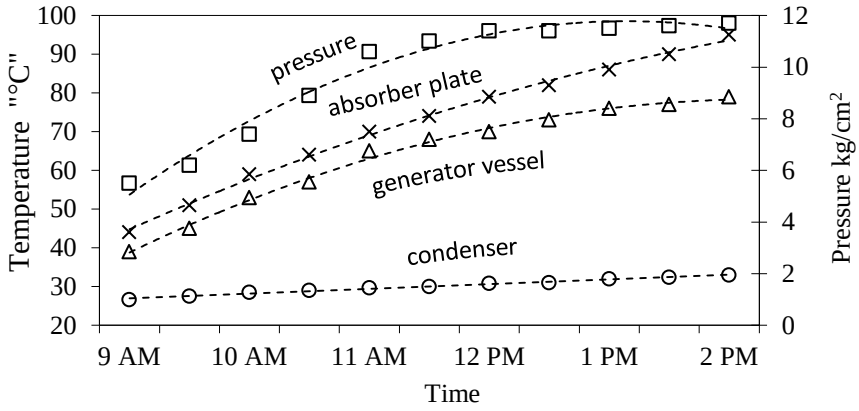

Figure 14: Heat transfer flow from FPC absorber plate through chilling system at different system pressureS.

Evaporator thermal performance and COP: Solar energy flows through the chilling system at different rates. System construction materials, system thermal insulations, fluids, and environmental factors are crucial in determining the system overall efficiency. Figure 15 demonstrates an efficiency comparison for the generator FPC, generator vessel, and for the condenser-evaporator, at different solar intensities. At average performance, the generator FPC deliverS a 14.3% of the total available solar energy in one day. While generator vessel passes 98% from the generator FPC energy or 13% from the total solar intensity to the condenser-evaporator section. Net energy of the condenser unit reached 55% form the energy delivered form generator vessel, and equals to 4.43 % from the total solar intensity (figs. 16 and 17).

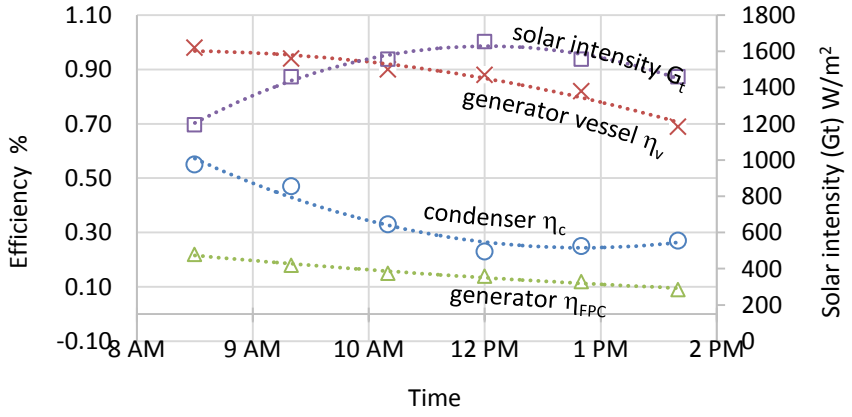

Figure 15: Chilling solar-assisted system efficiency at solar intensities during the daytime.

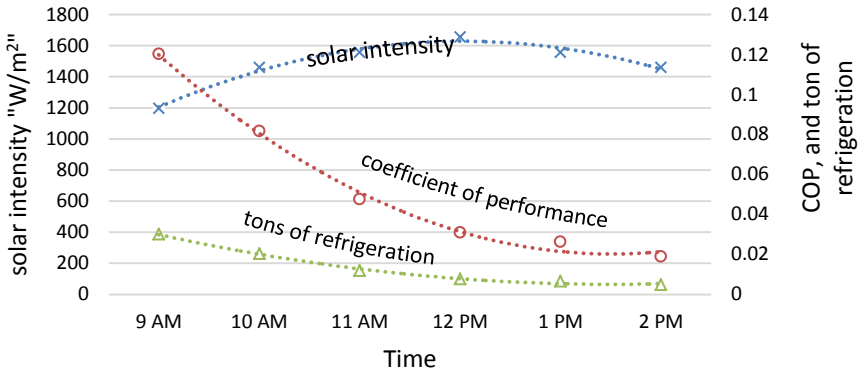

Figure 16: The coefficient of performance for the chilling solar-assisted system.

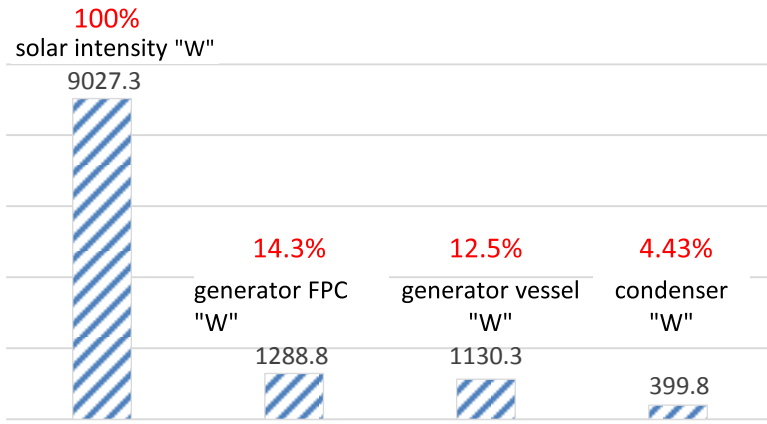

Figure 17: Energy transfer through generator FPC, generator vessel, and condenser.

The chilling-solar-assisted system coefficient of performance COP relationship, as found in figure 18, reached its maximum value at 0.12 (equivalent to 0.03 ton of refrigeration) and decreased as system temperature increased. Chilling solar-assisted system was able to reduce evaporator temperature form 30 °C to 4 °C within 100 minutes without load as illustrated in figure 19.

Field growing crops suffer from heat gain of respiration, and from the surrounding environment. Calculated heat load for one kilogram of potatoes showed increase of energy load form 25 W.h to 35.4 W.h with increasing ambient air temperature form 5 °C to 25 °C (fig. 20).

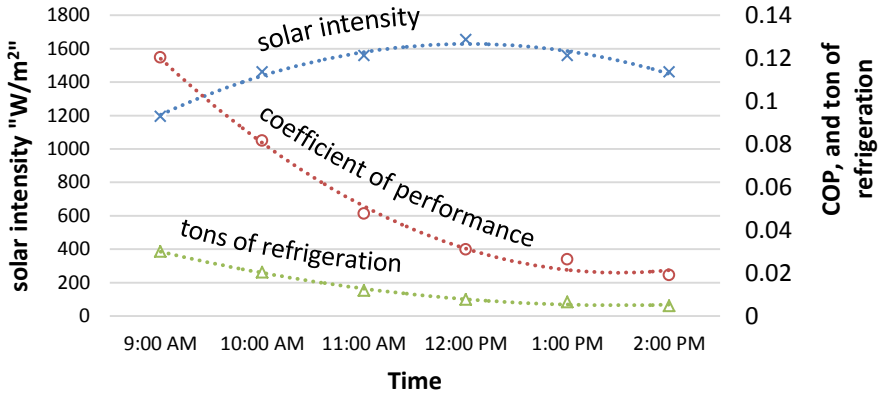

Figure 18: The coefficient of performance for the chilling solar-assisted system.

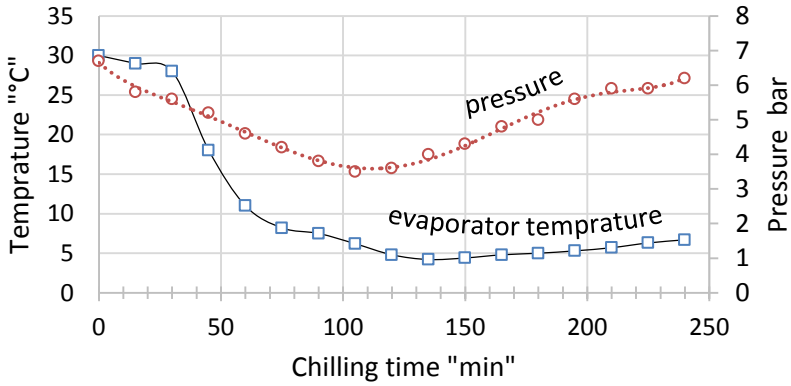

Figure 19: Required time for heat removal from the empty evaporator vs system pressure.

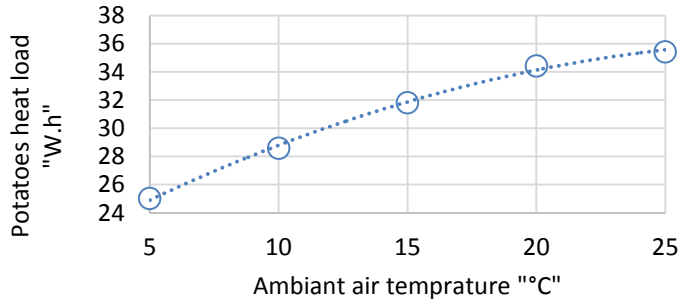

Figure 20: Calculated potatoes heat load at different ambient temperatures.

Chilling solar-assisted system was constructed for fast removal of crops' field heat. The system capacities will depend on the desired final temperature for safe transport of the crop. Figure 21, compares the net energy to remove form one kilogram of potatoes crop to reduce its

temperature from 30 °C to 4 °C. Summing up needed reduction of potatoes energy, cooling energy lost for surroundings, and potatoes respiration energies form integration of the area under curve in figure 22. It was found that cooling energy of one kilogram of potatoes will consume 119.65 W.h of the 399.8 W.h - evaporator available energy or 1.33% of the total solar intensity under the experimental conditions.

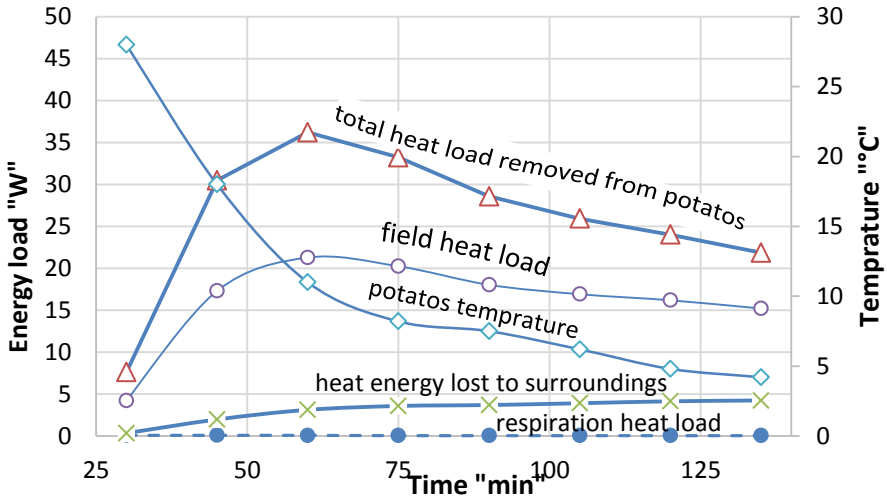

Figure 21: Potatoes thermal load energy and heat removal response.

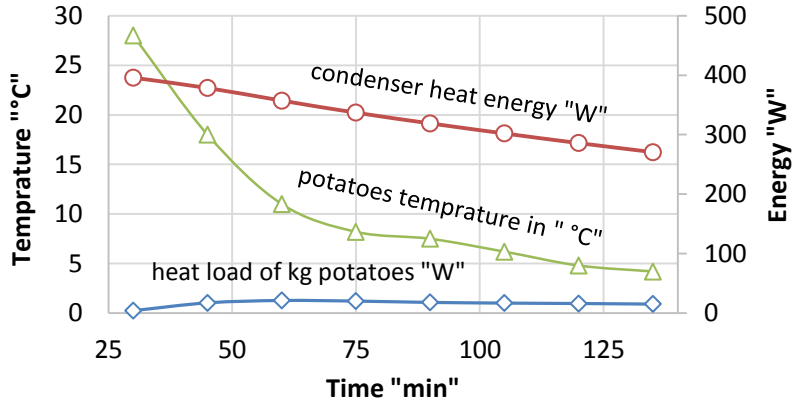

Figure 22: Calculated heat load removal from kilogram of potatoes and energy transfer from condensing to evaporating processes.

From figure 23, the evaporator capacity will be three kilograms of potatoes for temperature reduction form 30 °C to 5 °C, and 18 kilograms for temperature reduction form 30 °C to 20 °C.

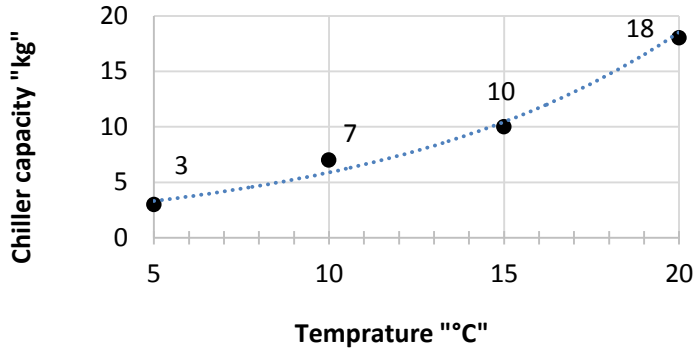

Figure 23: Chilling solar-operated potatoes holding capacities at different chilling temperature levels.

Chilling will take 45 minutes to reduce kilogram of potatoes from 30 °C to 20 °C and 120 minutes to reach 4 °C as seen in figure 24.

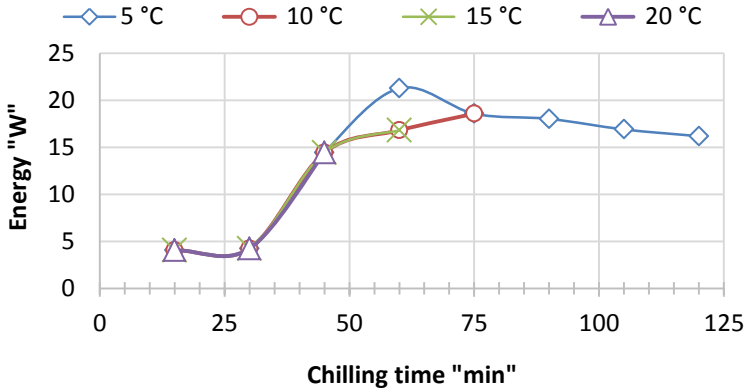

Figure 24: Required time for heat removal from potatoes at different temperature levels.

CONCLUSION

Solar-assisted chilling system is a simple and cheap system to build. It has a dual usage in post-harvest treatments, and can work as chiller or as a heater in many agricultural applications.Enables increased horticultural production both for domestic and export consumption. Generating additional income for smallholder farmers and increased access to nutritional fruits and vegetables while generating both manufacturing and service based employment.

Chilling system generator consisted of FPC with generator vessel. FPC optical efficiency **(**$\eta_0 = F_R\ (\tau\alpha)$) was 26% and varied according to ambient air temperature and the rate of fluid flow. The FPC average

efficiency under the experimental conditions was 13% at total solar intensity of 9027.26 W/m^2/day and air speed of 5.3 m/s. The lowest obtained temperature in evaporator was 3.2 °C.

The generator FPC overall heat removal coefficient **U** was 8.775 W/m^2. °C and the overall heat removal factor $\mathbf{F_R}$ was 0.3971. The FPC $\mathbf{F_R\ U_L}$ was 3.485 W/m^2 °C and found within the value for the **FPC** standard (3-8 W/m^2 °C). Further enhancement on optical efficiency must be made, by changing the plastic cover to non-iron glass cover. Focused and solar concentrator collectors are essential for large capacities of chilling load.

With 98% thermal efficiency, Generator **vessel** was able to deliver most of the collected thermal mass of the solar collector (about 12% of the total solar intensity per day. The generator vessel was able to withstand system pressure ranging from 3.4 to 12.5 bar.

Condenser-evaporator with 55% thermal efficiency was able to deliver 4.4% of the total solar intensity energy as chilling energy per cycle.

REFERENCES

Abdel Mawla H. A., A. M. El-Lithy, M. Z. Attar, and R. K. Mahmoud. 2012. Evaluation of flat-plate solar collector for agricultural applications. The 19th annual. Conf. of the Misr Soc. Agric. Eng.; Prospects of modern technology in agricultural engineering and management of environmental problems, (19):651-662.

Atanda, S., Pessu, P., Agoda, S., Isong, I., and Ikotun, I. 2011. The concepts and problems of post-harvest food losses in perishable crops. African Journal of Food Science, 5(11): 603–613.

Duffie, J. A., and Beckman, W. A. 1980. Solar engineering of thermal processes. NASA STI/Recon Technical Report A, 81: 16591.

Duffie, J. A., and Beckman, W. A. 2013. Solar engineering of thermal processes. John Wiley \& Sons.

Kalogirou, S. A. 2004. Solar thermal collectors and applications. Progress in energy and combustion science, 30(3): 231–295.

Kassem, A.; A.Shoker and A.Bassuony 1993, performance of an intermittent absorption solar refrigeration system. Misr J. Agric. Eng, 10 (2): 267-285.

Liberty, J., Okonkwo, W., and Echiegu, E. 2013. Evaporative Cooling: A Postharvest Technology for Fruits and Vegetables Preservation. International Journal of Scientific & Engineering Research, 4(8): 2257– 2266.

Lipinski, B., Hanson, C., Lomax, J., Kitinoja, L., Waite, R., and Searchinger, T. 2013. Reducing food loss and waste. World Resources Institute, Washington DC, Working Paper.

Owen, M. S., and Kennedy, H. E. 2009. Handbook: Fundamentals. American Society of Heating, Refrigeration, and Air-Conditioning Engineers.

Wessel, D. 2001. Ashrae fundamentals handbook 2001 (SI edition). American Society of Heating, Refrigerating, and Air-Conditioning Engineers, 31.

Yusuf, B. L., and He, Y. 2013. Design, development and techniques for controlling grains post-harvest losses with metal silo for small and medium scale farmers. African Journal of Biotechnology, 10(65): 14552–14561.

Cengel, Y. 2007. Introduction to Thermodynamics and Heat Transfer+ EES Software (Vol. 77235657). McGraw Hill Higher Education, London, ISBN.

El Masry, O. A. 2002. Performance of waste heat absorption refrigeration system. 6 th Saudi Eng. Conf. 5: 531–544.

Incropera, F. P., Lavine, A. S., and DeWitt, D. P. 2011. Fundamentals of heat and mass transfer. John Wiley & Sons.

Kalogirou, S. 2008. Recent patents in absorption cooling systems. Recent Patents on Mechanical Engineering, 1(1): 58–64.

Mansoori, G. A., and Patel, V. 1979. choice of working fluids for solar absorption cooling systems. Solar Energy, 22(6): 483–491.

Mittal, V., Kasana, K., and Thakur, N. 2005. The study of solar absorption air-conditioning systems. Journal of Energy in Southern Africa, 16(4): 59–66.

Ursula, E. 2003. Solar technologies for buildings. Great Britain: Antony Rowe Ltd.

Wang, S. K. 2000. Handbook of air conditioning and refrigeration.:1.12-1.13.

Whitman, W. C., Johnson, W. M., and Tomczyk, J. A. 2005. Refrigeration & air conditioning technology (SEVENTH EDITIO N., pp. 1–1690). Cengage Learning.

Bakker-Arkema, F. W., Baerdemaeker, J. de, Amirante, P., Ruiz-Altisent, M., Studman, C., and others. 1999. CIGR handbook of agricultural engineering, Volume 4: Agro-processing engineering. American Society of Agricultural Engineers (ASAE).(accessed at http://en.wikipedia.org/wiki/Absorption_refrigerator)

الملخص العربى

تطوير نموذج للتبريد بالطاقة الشمسية

رجب قاسم [١] و م. ز. العطار [٢]

عَمِدت الدراسة إلى تطوير نموذج للمعاملة الحرارية بالتبريد يستمد قدرته من الطاقة الشمسية بواسطة مجمع شمسى مسطح، بحيث يتميز بسهولة الإنشاء والصيانة مع توافر المواد والتكنولوجيات الخاصة بها محليا، واستخدام الطاقة الشمسية كمصدر للطاقة ولارتباطها على نحو وثيق بمتطلبات طاقة التبريد المطلوبة. فكلما زادت طاقة الإشعاع الشمسى وحرارة المنتج الزراعى، زاد الاحتياج للتبريد وزادت كفاءة تشغيل النموذج، وفى ظروف انخفاض معدلات التعرض الشمسى يقل الاحتياج للتبريد، وما يتبعه من انخفاض كفاءة النموذج بما لا يؤثر على كفاءة عمليات ما بعد الحصاد الحرارية إجمالاً.

يعمل النظام من خلال تمرير مخلوط التشغيل-المكون من نسب متساوية من الأمونيا والماء-فى (١) **المولد الحرارى** الذى يعمل خلال (أ) المجمع الشمسى المسطح بقدرة استخلاص طاقة حرارية من الإشعاع الشمسى ١٣٪ (في المتوسط تحت الظروف التجربة ولمساحة المجمع المعرضة ١,٩٥ م^{٢})، (ب) وحدة استيعاب وتخزين مخلوط التشغيل المسخن. حيث يتم تسخين سائل التشغيل ومن ثم يمر عبر (٢) أسطوانتين معدنيتين متداخلتين تعملان كمكثف ومبخر على التوالى. حيث تتم عملية **تكثيف** بخار المخلوط المركز بتمرير تيار من الماء البارد خلال الأسطوانة الخارجية فيتكثف البخار بالأسطوانة الداخلية. وفى مرحلة **التبخير**، يوقف تمرير مياه التبريد لإتاحة عمل النظام كمبخر ومن ثم خفض درجة حرارة المنتج الغذائي.

[١] **معيد بقسم الهندسة الزراعية، كلية الزراعة جامعة أسيوط**

[٢] **مدرس الهندسة الزراعية، كلية الزراعة جامعة عين شمس**

قُدِر معامل كفاءة المبرد الشمسى القصوى ٠,١٤ بما يعادل ٠,٠٣ طن تبريد، عند إشعاع شمسى ٩٠٢٧,٢٦ وات/م^{٢} لليوم، وحركة هواء ٥,٣ م/ث، مما خفض درجات الحرارة لتسجل ثلاثة درجات ونصف الدرجة المئوية (دون حمل حرارى).

أكدت الحسابات **المرجعية** لتبريد الحاصلات الزراعية، إمكانية استخدام النموذج المبدئى تبريد ثلاثة كيلوجرامات من درنات البطاطس من ٣٠°م إلى ٤°م، أو ما يعادل ثمانية عشرة كيلوجرامات من درنات البطاطس عند التبريد إلى ٢٠°م عند نفس ظروف التشغيل.

سُجلَت كفاءة وحدة الاستيعاب الحديدية لسائل التشغيل بالمولد نحو ٩٨٪، بما يساوى ١٢٪ من إجمالي طاقة الأشعة الشمسية الساقطة في اليوم. وقد أمكن لوحدة الاستيعاب من تحمل ضغوط التشغيل الواقعة في المدى ٣,٤ إلى ١٢,٥ ض. جوى. كما استخدمت وحدة تصحيح أعلى وحدة الاستيعاب لمنع المياه من الوصول إلى المكثف. بلغت كفاءة وحدة التكثيف – التبخير الحرارية ٥٥٪ من الطاقة الواردة إليها، وما يساوى ٤,٤ ٪ من إجمالي الطاقة الشمسية المجمعة في اليوم الواحد.

تُوصى الدراسة باستخدام المركزات الشمسية بدلا من المجمع المسطح لزيادة كفاءة عمليات التبريد وإتاحة الناتج الحرارى الجانبى فى التطبيقات المختلفة بالمزرعة. كما توصى الدراسة بتشييد حيز تبريد منفصل عن حيز التكثيف لإمكان الحصول على تبريد مستمر وتخفيض من فقد الحرارة بين عمليتى التبريد والتكثيف.